arXiv:1304.0399v1 [q-bio.NC] 1 Apr 2013

Synchronous activity patterns of a large neuronal network: a characterization by Causal Information Theory based tools

Emilia B. Deleglise [1,2], **Osvaldo A. Rosso** [3,4], **Fernando Montani** [1,2,*]

1: *IFLYSIB, CONICET, Universidad Nacional de La Plata,*
Calle 58, 789, (1900) La Plata, Buenos Aires, Argentina.
2: *Departamento de Física, Facultad de Ciencias Exactas,*
Universidad Nacional de La Plata (UNLP)
Calle 49 y 115, C.C. 67, (1900) La Plata, Buenos Aires, Argentina.
3: *Laboratorio de Sistemas Complejos, Facultad de Ingeniería,*
Universidad de Buenos Aires (UBA)
4: *LaCCAN/CPMAT - Instituto de Computação, Universidade Federal de Alagoas*
(UFAL) BR 104 Norte km 97, 57072-970 Maceió, Alagoas, Brazil.

April 2, 2013

Abstract

We consider a network of cortical spiking neurons with axonal conduction delays and spike timing dependent plasticity (STDP), which is representative of a cortical column or hypercolumn. Each neuron fires following a Hodgkin-Huxley like dynamics and it is interconnected randomly to another neurons. In this work we use a permutation entropy approach to characterize the dynamic of the spiking neural activity of a given population of neurons. This allow us to investigate the fine temporal structure of complex neuronal signals not just by using the probability distributions associated with inter-spike intervals, but instead considering much more subtle measures accounting for its causal structure.

Neural dynamics ; Permutation Entropy ; Complexity
PACS: 02.50.-r , 05.45. Tp , 87.19.La.

* *E-mail: fmontani@gmail.com*

1 Introduction

Detection of dynamical changes in complex systems is one of the most relevant issues in neuroscience. In the field of experimental neurophysiology, a magnitude used to analyze the network is the normalized variance of the probability distribution associated with the inter pikes intervals (ISI). Unfortunately the dynamic effects of the network cannot be fully captured by such simple calculations, and it does not provide therefore reliable dynamic information that can be tested in the phase space.

One of the simplest computational models of neurons is the Simple Model of Spiking Neurons by Izhikevich [1]. This model uses just a two-dimensional (2-D) system of ordinary differential equations and four parameters for generate twenty different types of neural dynamics. Our research is focused on biophysical properties of the Hodgkin-Huxley equations [2], but using the simple model of Izhikevich [1]. In order to investigate the dynamical properties of a population of neurons, we use a neural network capable of reproducing the main biological characteristics of brain oscillation patterns and spontaneous brain activity [3].

Brain dynamics variables are noisy, non-stationary, nonlinear and rife with temporal discontinuities. Moreover, due to the occurrence of noise and artifacts in various forms, it is often not easy to get reliable information from a series of measurements. Bandt and Pompe [4] have proposed a robust approach to time series analysis on the basis of counting ordinal patterns introducing the concept of permutation entropy for quantifying the complexity of a system behind a time series. Thus, it is considered the ordinal structure of the time series instead of the values themselves [5].

In this paper, we use an information-theory-based approach to investigate the causality within inter spikes intervals (ISIs). By estimating Fisher information versus MPR complexity [6, 7, 8] of the ISIs signals, we show that it is possible to quantify the optimal amount of interconnected neurons that maximizes information transmission within a biologically plausible neuronal network simulation. This approach provides, thus, dynamic information about the neural network that may play a crucial role in the rhythmic activity pattern in the brain, and in the processing of information.

2 Neuronal network simulation model

Neurons fire spikes when they are near a bifurcation from resting to spiking activity, and it is the delicate balance between noise, dynamical currents and initial condition what determines the phase diagram of neural activity. While there are a huge number of possible ionic mechanisms of excitability and spike generation, exist just four bifurcation mechanisms that can result in such a transition. That is, there are many ionic mechanisms of spike generation, but only four generic bifurcations of equilibria. These bifurcations divide neurons into four categories: integrators or resonators, monostable or bistable [9].

Bifurcation methodologies [9] allow us to reproduce accurately the biophysical properties of Hodgkin-Huxley neuronal models by just taking a two-dimensional system of ordinary differential equations and four different parameters. This model is named simple model of spiking neurons [1], and the system of ordinary differential equations reads:

$$v' = 0.04v^2 + 5v + 140.u + I \tag{1}$$

$$u' = a(bv - u) \tag{2}$$

with the auxiliary after-spike resetting

$$if \ v \geq +30mV, \quad then \quad \begin{cases} v \leftarrow c \\ u \leftarrow u + d. \end{cases} \tag{3}$$

Where v is the membrane potential of the neuron, and u is a membrane recovery variable, which accounts for the activation of $K+$ ionic currents and inactivation of $Na+$ ionic currents, and gives negative feedback to v. Thus we are just considering a two-dimensional (2-D) system of ordinary differential equations of two variables u and v, and all the known types of neurons can be reproduced by taking different values of the four parameters a, b, c, d. After the spike reaches its apex at +30 mV (not to be confused with the firing threshold) the membrane voltage and the recovery variable are reset according to Eq. (3). The variable I accounts for the inputs to the neurons [1]. Summarizing, each neuron can be described by a simple spiking model that allows us to reproduce the twenty most fundamental neuro-computational features of biological neurons [1].

Here, we consider a network simulation model in which the number for interconnected neurons is a parameter under control, and each neuron can be interconnected randomly with two neurons or more neurons [3]. The network simulation takes into account cortical spiking neurons with axonal conduction delays and spike-timing-dependent plasticity (STDP). The magnitude of the synaptic weight between pre- and postsynaptic neurons depends on the timing of the spikes according to the STDP rules [3]. Importantly, the interplay between conduction delays and STDP helps the spiking neurons to produce stable firing patterns that would not be possible without these assumptions. Each neuron in the network is described by the simple model of spiking neurons of [1] which has been described above in Eq. (1) to Eq. (3).

This model presents biologically plausible phenomena such as patterns of spontaneous cortical activity and brain wave like oscillations. Since we cannot simulate an infinite-dimensional system on a finite-dimensional lattice, we choose a large network with a finite-dimensional approximation taking a time resolution of 1 ms. To illustrate the simulation we take first a network consists of $n = 1000$ neurons with $n_e = 550$ being of excitatory regular (RS) spiking type, and the remaining $n_i = 450$ of inhibitory fast spiking (FS) type ($n = n_e + n_i$). Each excitatory regular spiking type neuron is connected to $m =$ 2,6,8, 10, 20, 30, 40, 50, 60, 70, 80, 90, 100, and 120 random neurons, so that the probability of connection is $m/n =$ 0.002, 0.006, 0.008,0.01,0.02,0.04,0.06,0.08,0.1 and 0.12. Each inhibitory fast (FS) spiking neuron is connected to $m =$ 2,6,8, 10, 20, 30, 40, 50, 60, 70, 80, 90, 100, and 120 excitatory neurons only. The second a network consists of $n = 900$ neurons with $Ne = 500$ being of excitatory (RS) type, and the remaining $ni = 400$ of inhibitory (FS) type ($n = n_e + n_i$). In this case, each excitatory regular spiking type neuron is connected to $m = 2$, 4, 6, 8, 10, 20,30,40,60,80,100 and 120 random neurons, so that the probability of connection is $m/n = 0.002$, 0.004,0.006,0.008,0.01,0.02,0.03,0.04,0.06,0.08,0.1 and 0.12. And each inhibitory (FS) neuron is connected to $m = 2$, 4, 6, 8, 10, 20,30,40,60,80,100 and 120 excitatory neurons only. In both cases synaptic connections among neurons have fixed conduction delays, which are random integers between 1 ms and 10 ms. The two network arrangement described above are representative of the general behavior shown by large network simulations taking the axonal conduction delays and spike-timing-dependent plasticity (STDP) approach. Although the pattern are random, reflecting connectivity within the cortex, one can implement sophisticated anatomy and the two sparse network being shown in this section are representative of a cortical column or hypercolumn [3].

3 Information Theory quantifiers

3.1 Shannon entropy, Fisher Information Measure and MPR - Statistical Complexity

Sequences of measurements (or observations) constitute the basic elements for the study of natural phenomena. In particular, from these sequences, commonly called time series, one should judiciously extract information on dynamical systems under study. We can defined an Information Theory quantifier as a measure that is able to characterize some property of the probability distribution function (PDF) associated with these time series. Entropy, regarded as a measure of uncertainty, is the most paradigmatic example of these quantifiers.

Given a time series $\mathcal{X}(t) \equiv \{x_t; t = 1, \cdots, M\}$, a set of M measures of the observable $\mathcal{X}$ and the associated PDF, given by $P \equiv \{p_j; j = 1, \cdots, N\}$ with $\sum_{j=1}^{N} p_j = 1$ and N the number of possible states of the system under study, the Shannon's logarithmic information measure [10] is defined by

$$S[P] = -\sum_{j=1}^{N} p_j \ln(p_j) \ . \tag{4}$$

This functional is equal to zero when we are able to predict with full certainty which of the possible outcomes j whose probabilities are given by p_j will actually take place. Our knowledge of the underlying process, described by the probability distribution, is maximal in this instance. In contrast, this knowledge is minimal, commonly, for a uniform distribution $P_e = \{p_j = 1/N, \forall j = 1, \cdots, N\}$.

The Shannon entropy S is a measure of "global character" that it is not too sensitive to strong changes in the PDF taking place on small-size region. Such is not the case with the Fisher's Information Measure $F[f] = \int \{|\vec{\nabla} f|^2/f\} \ dx$

[11, 12], which constitutes a measure of the gradient content of the distribution f (continuous PDF), thus being quite sensitive even to tiny localized perturbations. The Fisher's Information Measure can be variously interpreted as a measure of the ability to estimate a parameter, as the amount of information that can be extracted from a set of measurements, and also as a measure of the state of disorder of a system or phenomenon [12, 13], being its most important property the so-called Cramer-Rao bound. It is important to remark that the gradient operator significantly influences the contribution of minute local f-variations to Fisher information value, so that the quantifier is called a "local" one. Note that Shannon's entropy decreases with skewed distribution, while Fisher's information increases in such a case. Local sensitivity is useful in scenarios whose description necessitates appeal to a notion of "order" [6, 7, 8]. The concomitant problem of loss of information due to the discretization has been thoroughly studied (see, for instance, [14, 15, 16] and references therein) and, in particular, it entails the loss of Fisher's shift-invariance, which is of no importance for our present purposes.

For the Fisher Information Measure computation (discrete PDF) we follow the proposal of Ferri and coworkers [17] (among others)

$$F[P] \ = \frac{1}{4} \ \sum_{i=1}^{N-1} \ 2\frac{(p_{i+1}-p_i)^2}{(p_{i+1}+p_i)} \ . \tag{5}$$

If our system is in a very ordered state and thus is represented by a very narrow PDF, we have a Shannon Entropy $S \sim 0$ and a Fisher's Information Measure $F \sim F_{max}$. On the other hand, when the system under study lies in a very disordered state one gets an almost flat PDF and $S \sim S_{max}$ while $F \sim 0$. Of course, S_{max} and F_{max} are, respectively, the maximum values for the Shannon Entropy and Fisher Information Measure. One can state that the general behavior of the Fisher Information Measure is opposite to that of the Shannon Entropy [18].

It is well known, however, that the degree of structure present in a process is not quantified by randomness measures and, consequently, measures of statistical or structural complexity are necessary for a better understanding (characterization) the system dynamics represented by their time series [19]. The opposite extremes of perfect order (i.e.: a periodic sequence) and maximal randomness (i.e.: a fair coin toss) are very simple to describe because they do not have any structure. The complexity should be zero in these cases. At a given distance from these extremes, a wide range of possible degrees of physical structure exists. The complexity measure allows one to quantify this array of behavior [20]. In the present work we have considered the effective statistical complexity measure (SCM) introduced by Lamberti *et al.* [21], (also called MPR-complexity) since it is able to detect essential details of the dynamics.

This statistical complexity measure is defined, following the seminal notion advanced by López-Ruiz *et al.* [22], through the product

$$\mathcal{C}_{JS}[P] \ = \ \mathcal{Q}_J[P, P_e] \cdot \mathcal{H}_S[P] \tag{6}$$

of the normalized Shannon entropy

$$\mathcal{H}_S[P] \;=\; S[P]/S_{max} \tag{7}$$

with $S_{max} = S[P_e] = \ln N$, $(0 \leq \mathcal{H}_S \leq 1)$ and the disequilibrium $\mathcal{Q}_J$ defined in terms of the Jensen-Shannon divergence. That is,

$$\mathcal{Q}_J[P, P_e] \;= Q_0 \mathcal{J}[P, P_e] \tag{8}$$

with

$$\mathcal{J}[P, P_e] \;=\; S[(P + P_e)/2] - S[P]/2 - S[P_e]/2 \tag{9}$$

the above-mentioned Jensen-Shannon divergence and Q_0 a normalization constant $(0 \leq \mathcal{Q}_J \leq 1)$, equal to the inverse of the maximum possible value of $\mathcal{J}[P, P_e]$. This value is obtained when one of the components of P, say p_m, is equal to one and the remaining p_j are equal to zero. The Jensen-Shannon divergence, that quantifies the difference between two (or more) probability distributions, is especially useful to compare the symbolic composition between different sequences [23]. Note that the above introduced SCM depends on two different probability distributions, the one associated to the system under analysis, P, and the uniform distribution, P_e. Furthermore, it was shown that for a given value of $\mathcal{H}_S$, the range of possible C_{JS} values varies between a minimum $\mathcal{C}_{min}$ and a maximum $\mathcal{C}_{max}$, restricting the possible values of the SCM in a given complexity-entropy plane [24]. Thus, it is clear that important additional information related to the correlational structure between the components of the physical system is provided by evaluating the statistical complexity measure.

3.2 The Bandt-Pompe approach to the PDF determination

The study and characterization of time series $\mathcal{X}(t)$ by recourse to Information Theory tools assume that the underlying PDF is a priori given. Per contra, part of the concomitant analysis involves extracting the PDF from the data and there is no univocal procedure with which everyone agrees. Bandt and Pompe (BP), almost ten years ago, introduced a successful methodology for the evaluation of the PDF associated to scalar time series data using a symbolization technique [4]. For a didactic description of the approach, as well as, its main biomedical and econophysics applications, see [5].

The pertinent symbolic data are *(i)* created by ranking the values of the series and *(ii)* defined by reordering the embedded data in ascending order, which is tantamount to a phase space reconstruction with embedding dimension (pattern-length) D and time lag τ. In this way it is possible to quantify the diversity of the ordering symbols (patterns) derived from a scalar time series. Note that the appropriate symbol-sequence arises naturally from the time series and no model-based assumptions are needed. In fact, the necessary "partitions" are devised by comparing the order of neighboring relative values rather than by apportioning amplitudes according to different levels. This technique, as opposed to most of those in current practice, takes into account the temporal structure of the time series generated by the physical process under study. This feature allows us to uncover important details concerning the ordinal structure of the time series [25, 8, 26] and can also yield information about temporal correlation [27, 28]. It is clear that this type of analysis of time series entails losing some details of the original series' amplitude-information. Nevertheless, by just referring to the series' intrinsic structure, a meaningful difficulty reduction is indeed achieved by Bandt and Pompe with regards to the description of complex systems. The symbolic representation of time series by recourse to a comparison of consecutive ($\tau = 1$) or non-consecutive ($\tau > 1$) values allows for an accurate empirical reconstruction of the underlying phase-space, even in the presence of weak (observational and dynamical) noise [4]. Furthermore, the ordinal-pattern's associated PDF is invariant with respect to nonlinear monotonous transformations. Accordingly, nonlinear drifts or scalings artificially introduced by a measurement device will not modify the quantifiers' estimation, a nice property if one deals with experimental data (see, i.e., [29]). These advantages make the Bandt and Pompe methodology more convenient than conventional methods based on range partitioning (i.e.: PDF based on histogram).

Additional advantages of the method reside in *(i)* its simplicity (we need few parameters: the pattern length/embedding dimension D and the embedding delay τ and *(ii)* the extremely fast nature of the pertinent calculation-process [30]. The BP methodology can be applied not only to time series representative of low dimensional dynamical systems but also to any type of time series (regular, chaotic, noisy, or reality based). In fact, the existence of an attractor in the D-dimensional phase space is not assumed. The only condition for the applicability of the Bandt-Pompe methodology is a very weak stationary assumption (that is, for $k \leq D$, the probability for $x_t < x_{t+k}$ should not depend on t [4]).

To use the Bandt and Pompe [4] methodology for evaluating the PDF P associated to the time series (dynamical system) under study, one starts by considering partitions of the pertinent D-dimensional space that will hopefully "reveal" relevant details of the ordinal-structure of a given one-dimensional time series $\mathcal{X}(t) = \{x_t; t = 1, \cdots, M\}$ with embedding dimension $D > 1$ ($D \in \mathbb{N}$) and embedding time delay τ ($\tau \in \mathbb{N}$). We are interested in "ordinal patterns" of order (length) D generated by $(s) \mapsto \left(x_{s-(D-1)\tau}, x_{s-(D-2)\tau}, \cdots, x_{s-\tau}, x_s \right)$, which assigns to each time s the D-dimensional vector of values at times $s, s-\tau, \cdots, s-(D-1)\tau$. Clearly, the greater the $D-$value, the more information on the past is incorporated into our vectors. By "ordinal pattern" related to the time (s) we mean the permutation $\pi = (r_0, r_1, \cdots, r_{D-1})$ of $[0, 1, \cdots, D-1]$ defined by $x_{s-r_{D-1}\tau} \leq x_{s-r_{D-2}\tau} \leq \cdots \leq x_{s-r_1\tau} \leq x_{s-r_0\tau}$. In order to get a unique result we set $r_i < r_{i-1}$ if $x_{s-r_i} = x_{s-r_{i-1}}$. This is justified if the values of x_t have a continuous distribution so that equal values are very unusual. Thus, for all the $D!$ possible permutations π of order D, their associated relative frequencies can be naturally computed by the number of times this particular order sequence is found in the time series divided by the total number of sequences.

Consequently, it is possible to quantify the diversity of the ordering symbols (patterns of length D) derived from a scalar time-series, by evaluating the so-called permutation entropy, the permutation statistical complexity and permutation Fisher information measure (that Shannon's entropy, MPR - Statistical entropy and Fisher information measure special versions corresponding to the Bandt and Pompe-PDF). Of course, the embedding dimension D plays an important role in the evaluation of the appropriate probability distribution because D determines the number of accessible states $D!$ and also conditions the minimum acceptable length $M \gg D!$ of the time series that one needs in order to work with a reliable statistics [31].

With respect to the selection of the other parameter, Bandt and Pompe suggest to work with $4 \leq D \leq 6$ and specifically considered an embedding delay $\tau = 1$ in their cornerstone paper [4]. Nevertheless, it is clear that other values of τ could provide additional information. It has been recently shown that this parameter is strongly related, if it is relevant, with the intrinsic time scales of the system under analysis [32, 33, 34].

3.3 Causal information planes

The above introduced based Information Theory quantifiers $\mathcal{H}_S$, $\mathcal{F}$ and $\mathcal{C}_{JS}$ evaluated using Bandt and Pompe's PDF allow us to define three causality information planes: $\mathcal{H} \times \mathcal{C}$, $\mathcal{H} \times \mathcal{F}$ and $\mathcal{C} \times \mathcal{F}$. The causality Shannon–complexity plane, $\mathcal{H} \times \mathcal{C}$, is based only on global characteristics of the associated time series Bandt and Pompe PDF (both quantities are defined in terms of Shannon entropies), while the causality Shannon-Fisher plane, $\mathcal{H} \times \mathcal{F}$ and causality complexity–Fisher, $\mathcal{C} \times \mathcal{F}$, are based on global and local characteristics of the PDF. In the case of $\mathcal{H} \times \mathcal{C}$ the variation range is $[0, 1] \times [\mathcal{C}_{min}, \mathcal{C}_{max}]$ (with $\mathcal{C}_{min}$ and $\mathcal{C}_{max}$ the minimum and maximum statistical complexity values, respectively, for a given $\mathcal{H}_S$ value [24]), while in the causality $\mathcal{H} \times \mathcal{F}$ and $\mathcal{C} \times \mathcal{F}$ the range is $[0, 1] \times [0, 1]$ in both cases. These causal information planes have been profitable used to separate and differentiate amongst chaotic and deterministic systems [25, 8]; visualization and characterization of different dynamical regimes when the systems parameters vary [6, 7, 8]; time dynamical evolution [31]; identifying periodicities in natural time series [35]; identification of deterministic dynamics contaminated with noise [36, 37] and; estimating intrinsic time scales of delayed systems [32, 33, 34]; among other applications (see [5] and references therein).

4 Results and Discussion

In order to illustrate our method we run the simulation for 20000 ms taking a time resolution of 1 ms, which is enough to guarantee the condition $M >> D!$ to be satisfied. Figures 1 A and B show the spike rasters considering $N = 1000$ and $N = 900$, respectively, for a time window of $1000ms$. Figures 2 A and B show the interspikes intervals (ISIs) considering $N = 1000$ and $N = 900$, respectively, for the entire time we run the simulation. Note that the previous plots only confirm that the neurons within the model fires with millisecond precision and we cannot gain any significative information about the dynamic. Figures 3 A and B show the normalized variance $Rp = \sqrt{Var(t_p)}/ < t_p >$ of the ISIs for two different simulated systems. Note that increasing degree of inter-connectivity m implies greater data dispersion. Thus, this kind of analysis does not provide us any insight of how information might saturates as the degree of interconnectivy becomes bigger.

In the following we use the Bandt and Pompe [4] methodology for evaluating the PDF P associated to the time series, considering an embedded dimensionality $D = 6$ (with $\tau = 1$). This embedded dimensionality is enough to capture efficiently causality information of the ordinal structure of the time series [4]. Figures 4 A and B show Fisher information Eq.(5) versus the MPR complexity Eq.(8) for the same biophysical parameters used above. Notice that Figures 4 A and B present a maximum at $m = 50$ and $m = 30$, respectively, for $n = 1000$ and $n = 900$. A similar behavior can be observed in Figures 5 A and B, which show Fisher information Eq.(5) versus permutation entropy Eq.(7). Consequently, building a phase space Fisher versus MPR complexity (or Fisher versus permutation entropy) provides us an useful tool to detect and quantify the optimal biophysical values which allows the neural network to transmit information more efficiently.

A generic neuron receives inputs from over ten thousand other neurons through dendritic connections called synapses. These inputs produce transmembrane currents changing the membrane potential of the neuron. Synaptic currents are called postsynaptic potentials (PSP). Small currents produce small PSP; large currents cause significant PSP to be amplified by sensitive channels, and may change the voltage in the cell membrane. This can leads therefore to the generation of a action potential. While there is a great amount of ionic mechanisms that may explain the excitability and generation of firing an spike, there are only four bifurcation mechanisms that may explain the transition. If we consider the geometry of the phase space in these branches, we can understand many properties computational neurons, and the nature of the threshold. We can understand also how these properties relate to each other, why some are equivalent and mutually exclusive (see [9] for an exhaustive review).

Here, we use an alternative methodology when considering a large population of neurons, we shown that by building the phase space of Fisher information versus MPR complexity/permutation entropy it is possible to characterize the dynamic of the system, and to find the optimal values which maximize information transmission within a neuronal network.

It is expected that information should saturate when the number of neurons increases [38, 39]. However, very little is known about how it could saturate. Our current approach provides a novel methodology to respond how deal saturation with information taking a realistic neuronal network. The approach is not only important from a theoretical point of view; it might help determine which areas of the cortex could have a higher level of information, and to evaluate how causal interactions in neural dynamics would be modulated by behavior. We believe that this will become a very important tool for future research on the encoding capacity of biologically realistic neural networks.

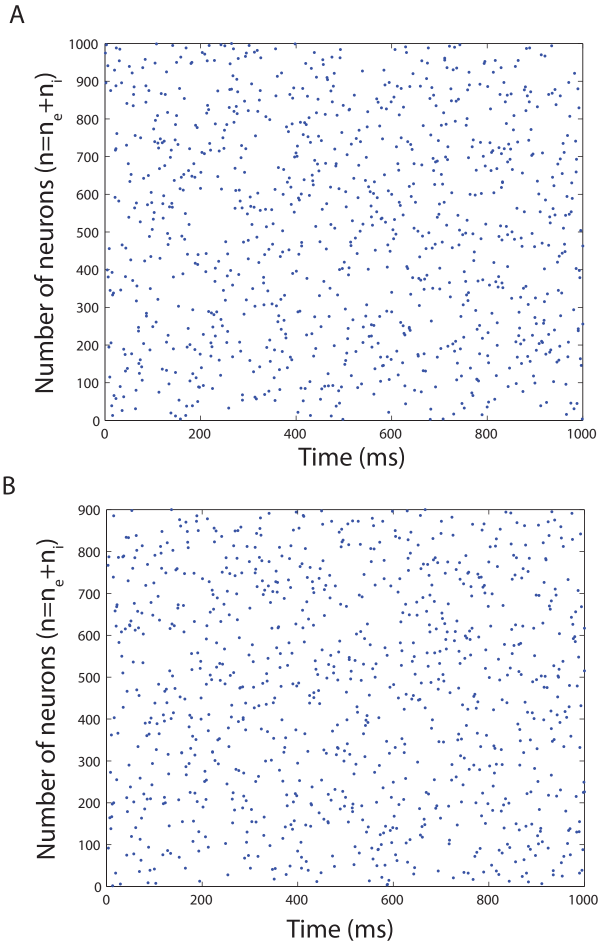

Figure 1: Spike rasters. ***A)*** $n = 1000$, $n_e = 550$, $n_i = 450$, $m = 50$ and taking a time window of $1000ms$ ***B)*** $n = 900$, $n_e = 500$, $n_i = 400$, $m = 30$ and taking a time window of $1000ms$.

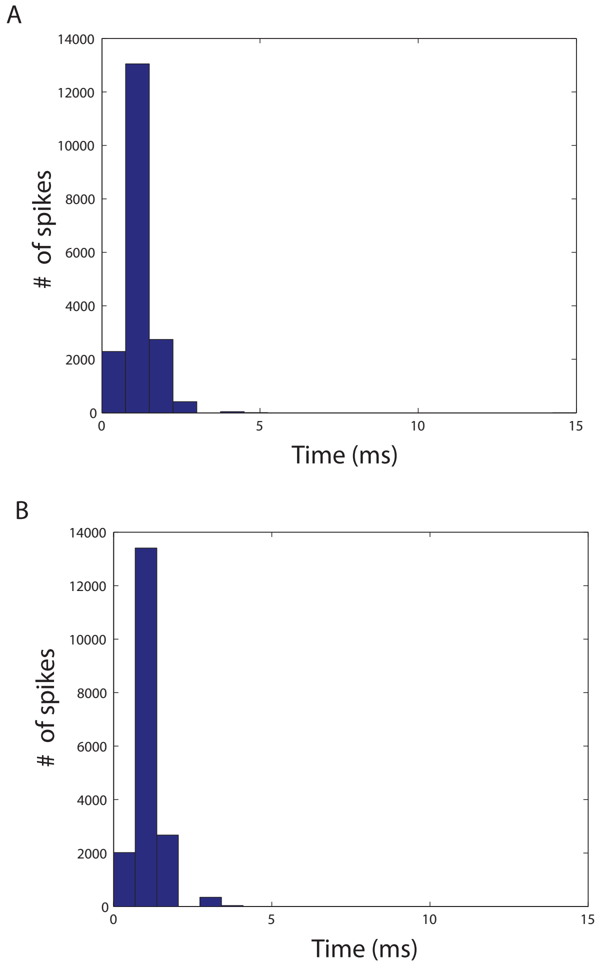

Figure 2: Histograms of the interspike intervals (ISIs). ***A)*** ISI for $n = 1000$, $n_e = 550$, $n_i = 450$ and $m = 50$. ***B)*** ISI for $n = 900$, $n_e = 500$, $n_i = 400$ and $m = 30$.

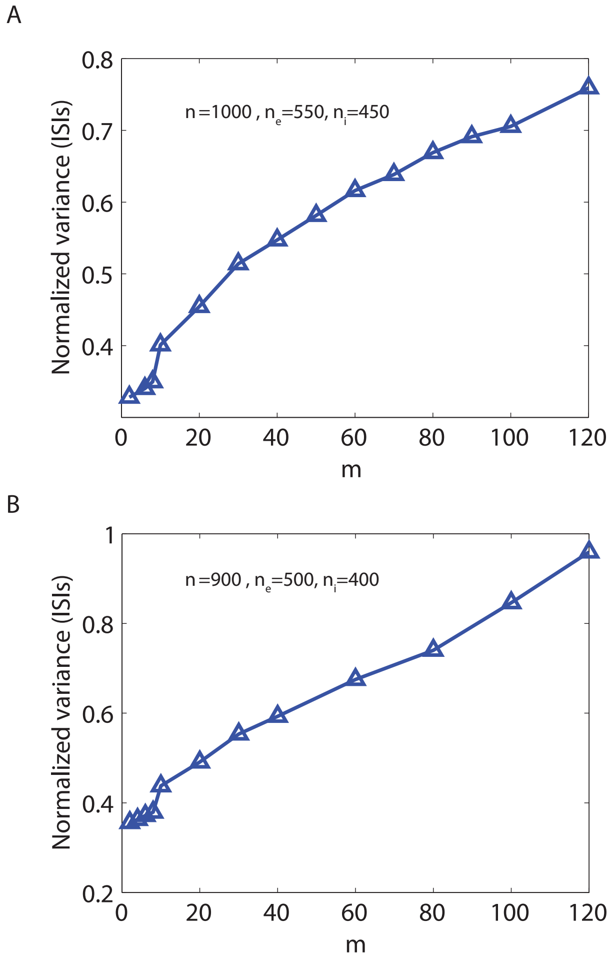

Figure 3: Normalized variance of the ISIs. ***A)*** $n = 1000$, $n_e = 550$, $n_i = 450$, and the points correspond to the different interconnectivities $m = 2$, 6, 8, 10, 20, 30, 40, 50, 60, 70, 80, 90, 100, and 120. ***B)*** $n = 900$, $n_e = 500$, $n_i = 400$, and the points correspond to the different interconnectivities $m = 2$, 4, 6, 8, 10, 20,30,40,60,80,100 and 120.

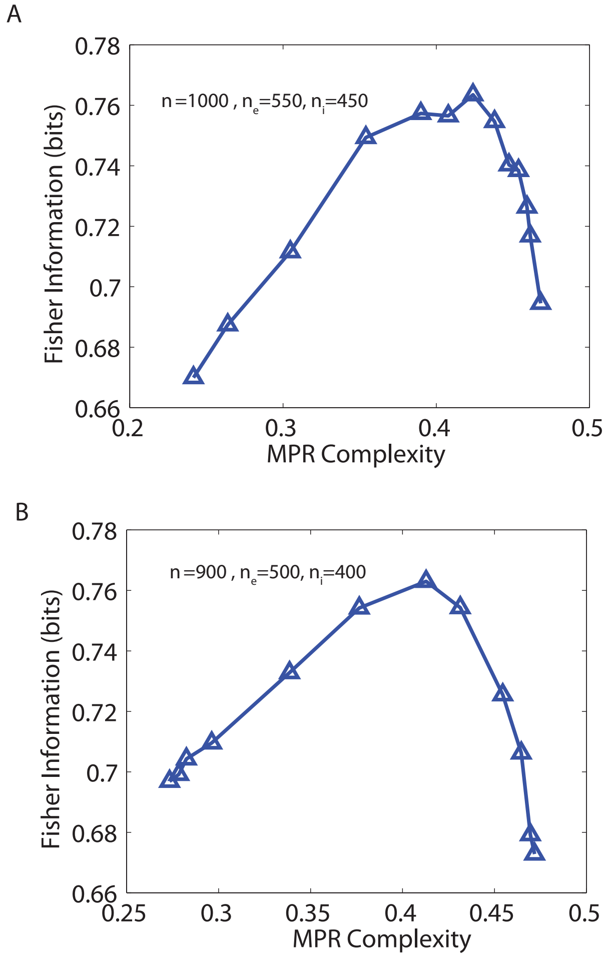

Figure 4: Fisher information versus MPR complexity, embedded dimensionality $D = 6$. ***A)*** $n = 1000$, $n_e = 550$, $n_i = 450$ and the points correspond to the different interconnectivities $m = 2,6,8$, 10, 20, 30, 40, 50, 60, 70, 80, 90, 100, and 120 (m gets bigger as the variable on the X-axis increases). The maximum value of Fisher information corresponds to $m = 50$. ***B)*** $n = 900$, $n_e = 500$, $n_i = 400$ and the points correspond to the different interconnectivities $m = 2$, 4, 6, 8, 10, 20,30,40,60,80,100 and 120 (m gets bigger as the variable on the X-axis increases). The maximum value of Fisher information corresponds to $m = 30$.

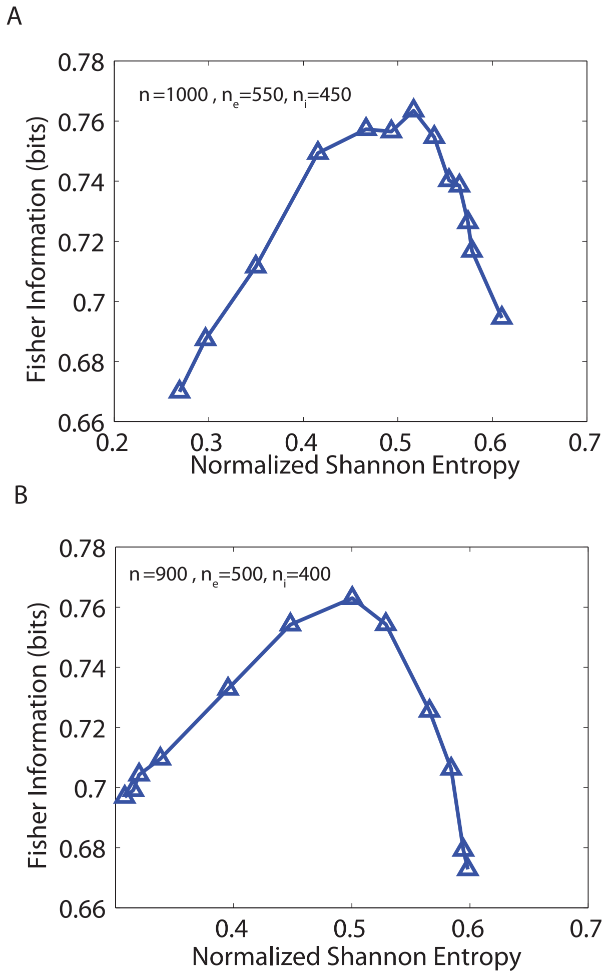

Figure 5: Fisher information versus normalized Shannon permutation entropy, embedded dimensionality $D = 6$. ***A)*** $n = 1000$, $n_e = 550$, $n_i = 450$ and the maximum value of Fisher information corresponds to $n = 50$. Same curve labels as in Fig. 4 A. ***B)*** $n = 900$, $n_e = 500$, $n_i = 400$ and the maximum value of Fisher information corresponds to $m = 30$. Same curve labels as in Figures 4B.

Acknowledgments

Research supported by PIP 0255/11 (CONICET). O. A. Rosso and F. Montani acknowledges support from CONICET, Argentina; also O. A. Rosso gratefully acknowledges support from CNPq, fellowship, Brazil.

References

[1] E. M. Izhikevich, IEEE Transactions on Neural Networks 14, 6 (2003).

[2] A. L. Hodgkin and A. F. Huxley, Journal of Physiology 117, 500 (1952) .

[3] E. M. Izhikevich, Neural Computation 18, 245 (2006).

[4] C. Bandt and B. Pompe, Phys. Rev. Lett. 88, 174102 (2002).

[5] M. Zanin, L. Zunino, O. A. Rosso, D. Papo, Entropy 14, 1553 (2012).

[6] O. A. Rosso, L. De Micco, A. Plastino and H. Larrondo, Physica A 389, 4604(2010).

[7] F. Olivares, A. Plastino and O. A. Rosso Physica A 391, 2518 (2012).

[8] F. Olivares, A. Plastino and O. A. Rosso Phys. Lett A 376, 1577 (2012).

[9] E. M. Izhikevich, *Dynamical Systems in Neuroscience: The Geometry of Excitability and Bursting*, The MIT press, Cambridge, Massachusetts (2007).

[10] C. Shannon, W. Weaver, *The Mathematical theory of communication*, University of Illinois Press, Champaign, Illinois (1949).

[11] R. A. Fisher, Philos. Trans. R. Soc. Lond. Ser. A 222, 309 (1922).

[12] B. Roy Frieden, *Science from Fisher information: A Unification.* Cambridge University Press, Cambridge (2004).

[13] A. L. Mayer, C. W. Pawlowski and H. Cabezas, Ecological Modeling 195, 72 (2006).

[14] K. Zografos, K. Ferentinos, T. Papaioannou, Canad. J. Stat. 14 (1986) 355.

[15] L. Pardo, D. Morales, K. Ferentinos and K. Zografos, Kybernetika 30, 445 (1994).

[16] M. Madiman, O. Johnson and I. Kontoyiannis, IEEE Int. Symp. Inform. Th., Nice, June 2007.

[17] G. I. Ferri, F. Pennini and A. Plastino. Phys. Lett. A 373, 2210 (2009).

[18] F. Pennini, A. Plastino, Phys. Rev. E 71, 047102 (2005).

[19] D. P. Feldman and J. P. Crutchfield, Phys. Lett. A 238, 244 (1998).

[20] D. P. Feldman, C. S. McTague, and J. P. Crutchfield, Chaos 18, 043106 (2008).

[21] P. W. Lamberti, M. T. Martin, A. Plastino, and O. A. Rosso, Physica A 334, 119 (2004).

[22] R. López-Ruiz, H. L.Mancini, and X. Calbet, Phys. Lett. A 209, 321 (1995).

[23] I. Grosse, P. Bernaola-Galván, P. Carpena, R. Román-Roldán, J. Oliver, and H. E. Stanley, Phys. Rev. E 65, 041905 (2002).

[24] M. T. Martín, A. Plastino, and O. A. Rosso, Physica A 369, 439 (2006).

[25] O. A. Rosso, H. A. Larrondo, M. T. Martín, A. Plastino, M. A. Fuentes, Phys. Rev. Lett. 99, 154102 (2007).

[26] O. A. Rosso, F. Oliavares, L.Zunino, L. De Micco, A. L. L. Aquino, A. Plastino, and H. A. Larrondo, EPJB 86, 116 (2012).

[27] O. A. Rosso and C. Masoller, Phys. Rev. E 79, 040106(R) (2009).

[28] O. A. Rosso and C. Masoller, European Phys. J. B 69, 37 (2009).

[29] P. M. Saco, L. C. Carpi, A. Figliola, E. Serrano and O.A. Rosso, Physica A 389, 5022 (2010).

[30] K. Keller, M. Sinn, Physica A 356, 114 (2005).

[31] A. Kowalski, M.T. Martín, A. Plastino, O. A. Rosso, Physica D 233, 21 (2007).

[32] L. Zunino, M. C. Soriano, I. Fischer, O. A. Rosso, and C. R. Mirasso, Phys. Rev. E 82, 046212 (2010).

[33] M. C. Soriano, L. Zunino, O. A. Rosso, I. Fischer, and C. R. Mirasso, IEEE J. Quantum Electron. 47, 252 (2011).

[34] L. Zunino, M. C. Soriano and O. A. Rosso, Phys. Rev. E 86, 046210 (2012).

[35] C. Bandt, Ecol. Modell. 182, 229 (2005).

[36] O. A. Rosso, L. C. Carpi, P. M. Saco, M. G. Ravetti, A. Plastino and H. Larrondo, Physica A 391, 42 (2012)

[37] O. A. Rosso, L. C. Carpi, P. M. Saco, M. G. Ravetti, H. Larrondo and A. Plastino, Eur. Phys. J B 85, 419 (2012).

[38] B. B. Averbeck, P. E. Latham, and A. Pouget, Nat. Rev. Neurosci. 7, 358 (2006).

[39] F. Montani, E. Phoka, M. Portesi, S. R. Schultz, Physica A, in press (2013) DOI:10.1016/j.physa.2013.03.012.